Food and Chemical Toxicology 129 (2019) 239–248

Contents lists available at ScienceDirect

Food and Chemical Toxicology

journal homepage: www.elsevier.com/locate/foodchemtox

Dibutyl phthalate impairs neural progenitor cell proliferation and hippocampal neurogenesis

Wonjong Lee[a], Jung-Hyun Cho[a], Yujeong Lee[a], Seulah Lee[a], Dae Hyun Kim[a], Sugyeong Ha[a], Yoshitaka Kondo[b], Akihito Ishigami[b], Hae Young Chung[a], Jaewon Lee[a,*]

[a] College of Pharmacy, Pusan National University, Busan, 46241, Republic of Korea
[b] Molecular Regulation of Aging, Tokyo Metropolitan Institute of Gerontology, Tokyo, Japan

ARTICLE INFO

Keywords:
Dibutyl phthalate
Hippocampal neurogenesis
Neural progenitor cell
Spatial learning and memory

ABSTRACT

Dibutyl phthalate (DBP) is commonly used plasticizer and a known endocrine disruptor that can cause birth defects and developmental disorders. Although several studies have reported that DBP has neurotoxic effects on neurite outgrowth and on learning and memory, its neurotoxic effects on neural progenitor cells (NPCs) have not been investigated. The present study was undertaken to determine the effects of DBP on NPCs and hippocampal neurogenesis. At high concentration DBP (500 μM) retarded NPC proliferation without affecting cell viability by arresting the cell cycle at G1 but did not cause cell death. DNA damage was observed by examining p53 expression and by γH2AX staining. DBP-treated cells had elevated ROS levels and exhibited mitochondrial dysfunction, which can cause DNA damage. Adult hippocampal neurogenesis was investigated using BrdU immunohistochemistry in young C57BL/6 mice intraperitoneally administrated with vehicle or DBP (10 or 50 mg/kg) for 2 weeks. DBP administered mice were found to have significantly fewer newly generated neurons in hippocampi, and the Morris water maze test revealed that DBP (50 mg/kg) impaired spatial learning and memory. Taken together, these findings suggest that DBP has harmful effects on NPCs and hippocampal neurogenesis and that DBP exposure could lead to learning and memory dysfunctions.

1. Introduction

Over the past half century, plastics have undoubtedly improved the quality of our lives, and today more than 200 million tons of plastics are produced globally each year (Thompson et al., 2009). Phthalates are esters of benzene dicarboxylic acids and are used in a wide range of industries (Koch and Calafat, 2009) as plastic plasticizers (Kamrin, 2009), and thus, phthalate exposure has inevitably increased in parallel with plastic production (Pivnenko et al., 2016). Phthalates increase the pliability and plasticity of plastics and are used in toys, pesticides, industrial dyes, food packaging materials, pharmaceuticals and in cosmetics and personal hygiene products (Schettler, 2006). Furthermore, phthalates such as di (2-ethylhexyl) phthalate (DEHP) and dibutyl phthalate (DBP) are not bound chemically to plastics and are easily released to air, water, and soil (Afshari et al., 2004). In particular, another author examined the DBP content of food samples randomly picked from the market in New York State. DBP was not detected in beverages and meat, but DBP was detected in milk, other dairy products, fish, grains, vegetable oils, seasonings and infant foods. That is, DBP was detected in food groups at 31% of frequencies (Schecter et al., 2013). Moreover, various types of phthalates have been identified in indoor dust and linked with allergies (Ait Bamai et al., 2016). In addition, phthalates can enter the human body when inhaled or even through skin and *in vivo* are metabolized variously depending on type. DBP has been reported to adversely affect liver, kidneys, fetuses, and developmental stages and to reduce anogenital distance in males, whereas DEHP has been reported to cause anovulation and to be toxic to testicular tissues (Hauser and Calafat, 2005). Phthalates are metabolized more rapidly than other environmental toxins and are hydrolyzed to mono-esters like mono (2-ethylhexyl) phthalate (MEHP), mono-benzyl phthalate (MBzP) and mono-butyl phthalate (MBP) and then released in urine and secretions (Hauser et al., 2004; Wormuth et al., 2006). The most widely used phthalates are DEHP, diisodecyl phthalate (DIDP), diisononyl phthalate (DINP), DBP, and benzyl butyl phthalate (BBP) (Wormuth et al., 2006), and their toxicities are classified by type, for example, diethyl phthalate (DEP) and DBP are classified as endocrine disruptors.

Exposure to DBP (500 mg/kg/day gestational diet) has been reported to reduce testicular testosterone levels and the expressions of genes involved in cholesterol transport and steroidogenesis (Struve

* Corresponding author.
E-mail address: neuron@pusan.ac.kr (J. Lee).

https://doi.org/10.1016/j.fct.2019.04.040
Received 21 January 2019; Received in revised form 3 April 2019; Accepted 22 April 2019
Available online 25 April 2019
0278-6915/

et al., 2009), and to impair immune cell function in human peripheral blood samples (Maestre-Batlle et al., 2018). Furthermore, DBP has been reported to change the structure of microbial communities to changes in the nitrogen cycle, glycolysis, the tricarboxylic acid (TCA) cycle, the pentose phosphate pathway, and in sulfuric acid metabolism (Xu et al., 2018). Recently toxicity studies showed DBP is a neurotoxin, for example, perinatal exposure to DBP was found to induce neuronal apoptosis and synaptic dysfunction in rats (Li et al., 2013) and in zebrafish (Xu et al., 2013). DBP has also been reported to caused primary neuronal cell death through aryl hydrocarbon receptors (Wojtowicz et al., 2017), to impair neuroplasticity via the Rho-GTPase signaling pathway (Ding et al., 2017), and to induce neurobehavioral problems in rats (Li et al., 2009), in mice (Farzanehfar et al., 2016), and in human (Kobrosly et al., 2014).

However, previous studies on the neurotoxicity of DBP were performed on fully differentiated neurons, and not on mitotic stem cells. Furthermore, it was recently reported bisphenol A and TBBPA (both endocrine disruptors) disrupt adult hippocampal neurogenesis (Cho et al., 2018; Jang et al., 2012; Lee et al., 2018; Tiwari et al., 2016). Accordingly, the present study was undertaken to evaluate the effects of DBP on NPCs and adult hippocampal neurogenesis.

2. Materials and methods

2.1. Reagents

Dibutyl phthalate (DBP), rotenone, antimycin A, carbonyl cyanide 3-chlorophenylhydrazone (CCCP), oligomycin, ribonuclease a (RNase A), MTT (3-[4,5-dimethyl-2-thiazolyl]-2,5-diphenyltetrazolium bromide), and corn oil were obtained from Sigma-Aldrich (MO, USA). 5-Bromo-2′-deoxyuridine (BrdU) was from ACROS Organics (Fair Lawn, NJ, USA). tetramethylrhodamine ethyl ester (TMRE), Alexa Flour 488, Alexa Flour 568, propidium iodide (PI), Hoechst 33342, and 2′-7′-dichlorofluorescein diacetate (DCF-DA) were purchased from Invitrogen (Eugene, OR, USA). Western blot detection reagent and enhanced chemiluminescence (ECL) solution were from Advansta Inc (Menlo Park, CA, USA). 6-Hydroxy-2,5,7,8-tetramethylchroman-2-carboxylic acid (trolox) and N-acetylcysteine (NAC) (both antioxidants) were purchased from Sigma-Aldrich and used at concentrations of 100 μM and 1 mM, respectively.

2.2. Cell line

The C17.2 cells used in this experiment were mouse-derived pluripotent neural progenitor cells (NPCs) isolated from cerebella and immortalized by viral mycosis (Snyder et al., 1992). NPCs were separated at intervals of 2–3 days, re-inoculated into 100-mm cell culture dishes, and cultured in a 5% CO_2 environment at 37°C. The medium used was Dulbecco's Modified Eagle's Medium (DMEM) 1× containing D-glucose 4,500 mg/L, sodium pyruvate 110 mg/L and L-glutamine 584 mg/L (LM 001–05 DMEM; Welgene, Daegu, South Korea). Toxicity experiments were conducted using complete DMEM one day after cell seeding.

2.3. Cell proliferation assay

The effects DBP on NPC proliferation were investigated using a germ cell analyzer (JULI™ Br; NanoEnTek Inc., Seoul). NPCs were seeded for a day in 60-mm dishes at 2×10^5 cells per dish and then observed for 24 h after DBP (500 μM) treatment. JULI™ Br images of NPCs were recorded at 10 min intervals.

2.4. Cell viability assay

A MTT assay was used to measure cell viability, as previously described (Riss et al., 2015). Briefly, NPCs (1×10^5 cells/ml) were seeded into 96-well plates and 24 h later treated with DBP (100, 250 or 500 μM) for up to 72 h. Media were then completely removed, 0.5 mg/ml MTT solution in 200 μl PBS was added to each well, and cells were incubated for 4 h at 37 °C. After removing the MTT solution, cells were lysed with a solubilizing solution (ethanol/DMSO (1:1)) and amounts of formazan produced were quantified by measuring absorbance at 560 nm using an ELISA microplate reader.

2.5. Quantitative detection of apoptosis

NPCs were seeded into 60-mm dishes, treated with 500 μM DBP for 6 h, collected, and stained with PI/Annexin V using the Annexin V-FITC Apoptosis Detection Kit (BD Biosciences, San Jose, CA). Cell death rates were determined by flow cytometric analysis (FACS).

2.6. Western blot analysis

NPCs were seeded into 60-mm plates and treated with DBP until 6 h. After experimental treatments, homogenates were solubilized in sodium dodecyl sulfate (SDS)-poly arcylamide gel electrophoresis (PAGE), and Protein concentrations were determined using a Bio-Rad (Hercules, CA) assay kit using bovine serum albumin (BSA) as the standard. Samples (20 μg protein/lane) were separated by 10% SDS-PAGE, and transferred to Immobilon-P^{SQ} transfer membranes (Millipore Corp., MA, USA), which were washed with TBS-T (Tris-HCl-based buffer containing 0.2% Tween 20 (pH7.5)), blocked with 5% skim milk in TBS-T for 30 min, and then incubated with the following primary antibodies: anti-Bax (1:1,000), anti-PARP (1:1,000), anti-caspase 3 (1:1,000), anti-cleaved caspase 3 (1:500), anti-p53 (1:500; all from Cell Signaling, MA), anti-cyclin D1, anti-cyclin E (both from Santa Cruz Biotechnology, Inc., CA) or anti-β-actin (1:10,000; Sigma-Aldrich Co., MO) in TBS-T at 4°C overnight. On following days, membranes were washed and incubated with secondary monoclonal anti-mouse (1:10,000) antibody or polyclonal anti-rabbit (1:10,000) antibody (both from Santa Cruz Biotechnology) in TBS-T at room temperature for 2 h. Blots were detected by ECL using a cooled CCD camera system (ATTO Ez-Capture II; Atto Corp., Tokyo).

2.7. Cell cycle detection analysis

NPCs were seeded, treated with 500 μM DBP for 6 h, washed twice with PBS, fixed with 70% ethanol at −20°C, rewashed with PBS, incubated with RNase for 30 min at room temperature, and treated with PI solution (0.1 μg/ml). DNA contents were determined by FACS.

2.8. ROS (Reactive oxygen species) production measurements

NPCs (5×10^3 cells/ml) were seeded in black 96-well plates and pretreated with DBP (500 μM) for 6 h. The medium was the removed and cells were incubated with 80 μM DCF-DA at 37°C for 30 min, and washed twice. Changes in fluorescence intensity at 10 min after DBP treatment were measured using a fluorescence plate reader (GloMax, Promega, Madison, WI).

2.9. Measurement of cellular mitochondrial respiration

The Seahorse XF (extracellular flux) Cell Mito Stress Test (Seahorse, Agilent Technologies, Santa Clara, CA) was performed according to the manufacturer's instructions. In brief, NPCs were cultured in XF cell culture microplate (1×10^5 cells per well) and treated with DBP and trolox for 6 h. Oligomycin (1 μM), CCCP (1 μM), and rotenone (0.5 μM) combined with antimycin A (0.5 μM) were injected sequentially through ports in the Seahorse Flux Park cartridges. Medium (supplemented with 25 mM D-glucose, 0.23 mM sodium pyruvate, and 500 μM L-glutamine, and the pH 7.4) for oxygen consumption rate measurement was prepared.

2.10. Mitochondrial membrane potential (MMP) analysis

MMP were measured using TMRE, which is a cell permeable, cationic, red fluorescent dye used to quantify intensity. NPCs were treated with 500 μM DBP for 6 h and then incubated in TMRE solution (0.05 μM in DMEM medium) at 37°C for 20 min. Mitotracker red, which accumulates red fluorescent dyes according to the membrane potential of living mitochondria, was also used. After DBP treatment, NPCs were incubated with mitotracker dye (final concentration 100 nM) at 37°C for 30 min. Representative images were obtained using an FV10i Flouview confocal microscope (Olympus, Tokyo, Japan).

2.11. Immunocytochemistry

NPCs were seeded in glass-bottomed dishes in a humidified 5% CO_2/95% air atmosphere at 37°C. The following day, cells were treated with DBP for 6 h, washed with PBS, fixed with 4% paraformaldehyde (PFA) in PBS for 15 min at 37°C, blocked with TBS-TS for 30 min, and incubated with primary antibody (anti-γ-H2AX; 1: 500; Cell Signaling, MA) at 4°C overnight. The following day, cells were washed, incubated with anti-mouse IgG labeled with Alexa Fluor 568 (3 μl/ml) for 3 h at room temperature, washed with TBS-TS, and incubated in 4',6-diamidino-2-phenyl-indole; a nuclear dye (DAPI) solution (1 μg/ml) at room temperature for 10 min. Images were acquired using a FV10i FLUOVIEW confocal microscope (Olympus).

2.12. Animals and housing

Male C57BL/6 mice were obtained from Daehan Biolink Co. Ltd. (Chungbuk, Korea) and housed at 20–23°C under a 12-h light/dark cycle with free access to food and water. Animals were randomly divided into three groups, i.e., the vehicle or the 10 or 50 mg/kg bw (body weight) DBP groups (n = 5 animals per group) and acclimatized for 1 week prior to administering DBP, which was administered intraperitoneally (i.p.) at 10 or 50 mg/kg bw for 2 weeks. Animals in the vehicle received the same volume of corn oil for 2 weeks. BrdU (100 mg/kg bw, i.p.) was administered during the last three days of the 2-week treatment period. The animal protocol used was reviewed and approved beforehand by the Institutional Animal Care Committee of Pusan National University (PNU-IACUC # PNU-2017-1008).

2.13. Tissue preparation

For histological studies, mice were anesthetized with diethyl ether, perfused intracardially with 0.9% NaCl in 0.1 M PBS (pH 7.4), and fixed by 0.1% M PBS in 4% PFA perfusion. Brains were then removed, placed in fixative solution at 4°C overnight, cryoprotected in 30% sucrose, and sectioned at 40 μm in the coronal plane using a freezing microtome (MICROM, Walldorf, Germany). Sections were stored at 4°C in Dulbecco's phosphate-buffered saline (DPBS) solution containing 0.1% sodium azide. For biochemical analysis, hippocampi were removed, frozen in liquid nitrogen, and stored at −80°C until needed.

2.14. BrdU DAB staining

To detect newborn cells, free-floating brain sections were treated with 0.6% H_2O_2 solution in Tris-buffered saline (TBS) to block endogenous peroxidase and incubated for 2 h at 65°C in 50% formamide/50% citric acid. Next, The DNA was denatured with HCl for 30 min at 37°C. Sections were blocked for 30 min in TBS-TS and neutralized by exposure to 0.1 M borate buffer (pH 8.5) for 15 min and incubated with primary antibody against BrdU (Abcam, Cambridge, MA) at 4°C with TBS-TS. Next day, tissues were treated with biotinylated secondary goat anti-mouse IgG antibody (3 μl/ml, Vector Laboratories, Burlingame, CA, USA) for 3 h at room temperature with ABS solution (avidin-peroxidase complex, Vectastain ABC reagent Elite Kit, Vector Laboratories). Next step was dyed with diaminobenzidine (DAB) solution for 5 min, and mounted with cover glass. Images were got on film using a Nikon ECLIPSE TE 2000-U microscope (Nikon). BrdU-positive cells were calculated every sixth section over the entire rostro-caudal extents of the hippocampus. The granular cell layer of the dentate gyrus (DG) was used as a reference area. All cell counts were performed by the same blinded researcher.

2.15. Double immunohistochemistry (IHC)

Brain sections were blocked with TBS-TS at room temperature for 30 min and incubated with primary antibodies; anti-BrdU (1:500, Abcam, MA), anti-DCX (1:500; Cell Signaling, MA), anti-GFAP (1:500; Cell Signaling, MA) and anti-Iba-1 (1:500; Wako, Tokyo, Japan) in TBS-TS at 4°C overnight. The next day, sections were washed with TBS and incubated with anti-mouse IgG labeled with Alexa Fluor 488 (3 μl/ml) and anti-rabbit IgG labeled with Alexa Flour 568 (3 μl/ml) for 3 h at room temperature. Representative images were obtained using an FV10i FLUOVIEW confocal microscope (Olympus, Tokyo).

2.16. Morris water maze test

Morris water maze (MWM) testing was performed as previously described (Shukitt-Hale et al., 2007). This test is typically used to investigate the effects on spatial learning and memory. Mice were forced to find a hidden platform (10 cm diameter) 1 cm beneath the surface of a pool (diameter 120 cm, height 32 cm) of opacified water maintained at 23–25°C. Mice underwent testing on 6 consecutive days after the 2-week treatment period. At the beginning of each session, a mouse was immersed in the pool at one of three randomly assigned starting positions (in the center of a quadrant not containing the platform). Mice were given 60 s to find the platform, when unsuccessful mice were guided to the platform and allowed to stay on it for 5 s. Attempts were videoed and analyzed using swimming path image tracking software (Noldus EthoVision® XT, Noldus Information Technology, Wageningen, Netherlands). Latencies (secs; times taken to find the platform), path lengths (cm), and swimming speeds (cm/s) were recorded.

2.17. Statistical analysis

The significances of intergroup differences were determined by ANOVA (analysis of variance) and Fisher's PLSD (protected least significant difference) test. P values of < 0.05 were considered statistically significant. The analysis was performed using Statview software (Version 5.0.1., SAS Institute Inc., Cary, NC).

3. Results

3.1. DBP reduced NPC proliferation rates but did not induce apoptosis

A JuLI Br Live Cell Analyzer was used to investigate the effects of DBP on NPCs (Fig. S1). While control cells normally proliferated around 26%–80%, DBP impaired cell proliferation which decreased from 80% to 40% of confluence. A representative image was captured after 6 h of DBP treatment (Fig. 1A). NPC proliferation of control and DBP treated cells was also assessed using the MTT assay up to 72 h. At high concentration (500 μM), DBP significantly reduced NPCs proliferation as compared with the control group (Fig. 1B). FACS, western blotting, and PI/Hoechst 33342 staining were used to determine whether DBP induce NPC death. Annexin V/PI staining showed DBP at the concentrations examined did not induce apoptosis or necrotic cell death (Fig. 1C). Furthermore, caspase 3, PARP, and Bax proteins (all apoptotic proteins) expressions were observed in NPCs treated with DBP, but no difference was observed between control and DBP groups (Fig. 1D). Furthermore, DBP reduced cell numbers but did not change PI stain intensities (pink) (Fig. 1E).

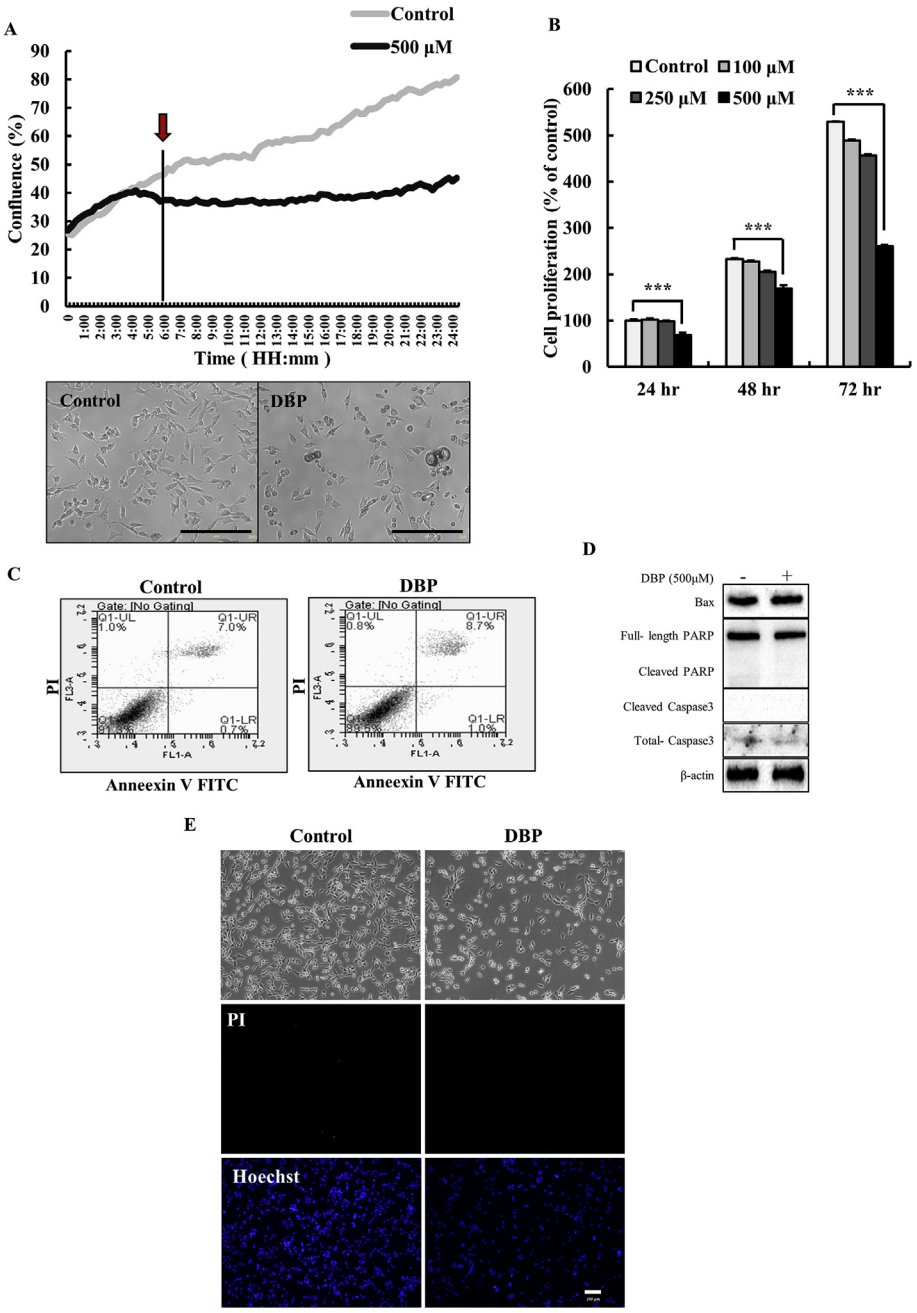

Fig. 1. Cell proliferation was reduced by DBP without affecting cell survival. (A) Measurement of proliferation rate using JuLI Br Live Cell Analyzer and representative image of NPCs at 6 h after treatment with DBP. Scale bar = 250 μm. (B) MTT assays showed NPCs proliferation reduced under DBP treatment. Results are presented as means ± standard errors (n = 8). (C) FACS analysis of apoptosis in NPCs. (D) Western blot analysis was performed to assess the expressions of apoptosis marker proteins. A representative blot from three independent experiments that yielded similar results is shown. (E) PI and Hoechst 33342 staining were used to detect necrotic NPCs. Scale bar = 100 μm. $^{***}p < 0.001$ vs. control (ANOVA with Fisher's PLSD procedure).

3.2. Analysis of cell cycle arrest

FACS showed an increase of ~11% in the G1 phase after 6 h of 500 μM DBP treatment. No difference was observed between control and DBP groups in terms of S phase and G2/M phase proportions (Fig. 2A and B). However, levels of cyclin D1 (regulates cell cycle progression in the G1 phase) were reduced by DBP. On the other hand, there was no change in the cyclin E required for the transition from the G1 to the S phase of the cell cycle (data not shown). Interestingly, though levels of apoptotic markers were not changed by DBP, p53 expression was increased (Fig. 2C and D). Senturk et al. reported that elevated p53 expression is the response to DNA damage (Senturk and Manfredi, 2013), and thus, γH2AX (a DNA damage marker) and DAPI (a nuclear stain) double-staining was performed to determine whether DBP-induced ROS caused DNA damage in NPCs. These results suggested p53 induction was significantly associated with DNA damage (Fig. 2E). Summarizing, these results showed cells underwent initial G1 arrest within 6 h of being exposed to DBP, and that this response required p53 activity. In addition, they suggested DBP-induced DNA damage leads to cell cycle arrest.

3.3. DBP induced ROS generation and mitochondria dysfunction

Previous studies have shown DBP increases ROS levels in primary neurons (Wojtowicz et al., 2017), and it has been reported G1 cell cycle arrest was induced at elevated ROS levels in mouse endothelial cells (Xiao et al., 2015). To determine whether these results hold for NPCs, ROS levels were assessed after treating cells with different concentrations of DBP for 6 h (Fig. 3A), and TMRE staining was used to determine effects on mitochondrial membrane potentials. TMRE staining intensity was significantly lower in 500 μM DBP-treated NPCs than in control, indicating that at this DBP concentration caused mitochondrial dysfunction (Fig. 3B). To confirm its effects on mitochondria, Seahorse Extracellular Flux (XF) analysis of oxygen consumption rate was

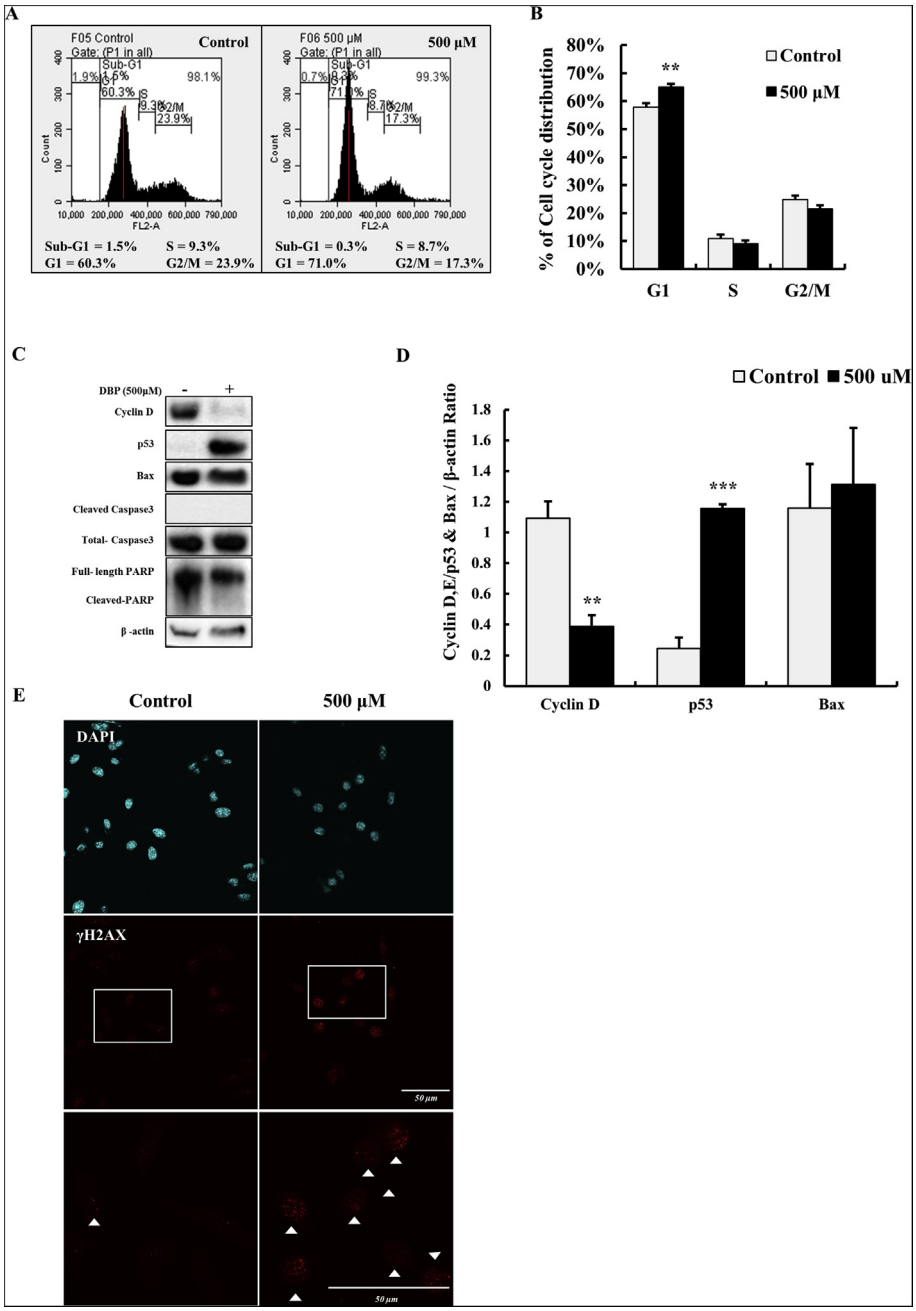

Fig. 2. DBP induced G1 phase arrest and increased p53 expression in NPCs. (A and B) FACS cell cycle analysis of 500 μM DBP treated NPCs and control. Results are presented as means ± standard errors (n = 9). (C and D) Western blot analysis was performed to investigate changes in the expressions of cell cycle arrest and apoptosis marker proteins. A representative blot from four independent experiments that yielded similar results is shown. Results are presented as means ± standard errors (n = 4). (E) Fluorescence image of DNA damage in NPCs caused by intracellular oxidative stress. DNA damage was assessed using γH2AX by ICC (white arrowheads indicate DNA damage). Scale bar = 50 μm. Cell cycle arrest due to DNA damage. $^{**}p < 0.01$ and $^{***}p < 0.001$ vs. control (ANOVA with Fisher's PLSD procedure).

performed. According to observed data, basal respiratory rate, spare respiratory capacity, ATP-linked breathing, proton leakage, maximal respiration, and non-mitochondrial oxygen consumption were significantly reduced by DBP in NPCs (Fig. 3C). These results suggest that DBP induces ROS production and mitochondrial dysfunction in NPCs.

3.4. Oxidative stress was involved in DBP-induced cell cycle arrest

Effects of antioxidants on G1 cell cycle arrest by DBP were investigated. Growth rates of NPCs co-treated with DBP and the antioxidants NAC or trolox were determined using the MTT assay. Treatment with DBP alone reduced cell proliferation, but antioxidant co-treatment blocked the DBP-induced cell cycle arrest (Fig. 4A). In addition, trolox was effective to block the altered expressions of cyclin D and p53 in NPCs by DBP (Fig. 4B and C). To further examine the effects of antioxidant co-treatment in mitochondrial function, we used XF analysis and immunofluorescence analysis using mitotracker. XF showed trolox co-treatment protected cells against DBP-induced reductions in basal respiration, ATP production, and maximal respiration (Fig. 4E and F), and immunofluorescent staining analysis using mitotracker showed trolox protected cells against DBP-induced reductions in mitochondrial membrane potential (Fig. 4D). Taken together, these results show DBP induced ROS-dependent cell cycle arrest (Fig. 4G).

3.5. DBP impaired hippocampal neurogenesis in adult mice

To determine the effect of DBP on hippocampal neurogenesis, male C57BL/mice (5 weeks old) were treated with DBP (10 or 50 mg/kg bw, i.p., daily) or vehicle for 2 weeks. For the proliferation study, BrdU was administered i.p. for 3 days from post-natal day (PND) 53–55 to label newly generated cells in hippocampi. In addition, behavioral tests were conducted from PND 55 (Fig. 5A). DBP 10 and 50 mg/kg bw treated mice showed significant decreases in numbers of newly-generated cells in the DG (Fig. 5B and C). In addition, IHC was performed using Iba-1 (a

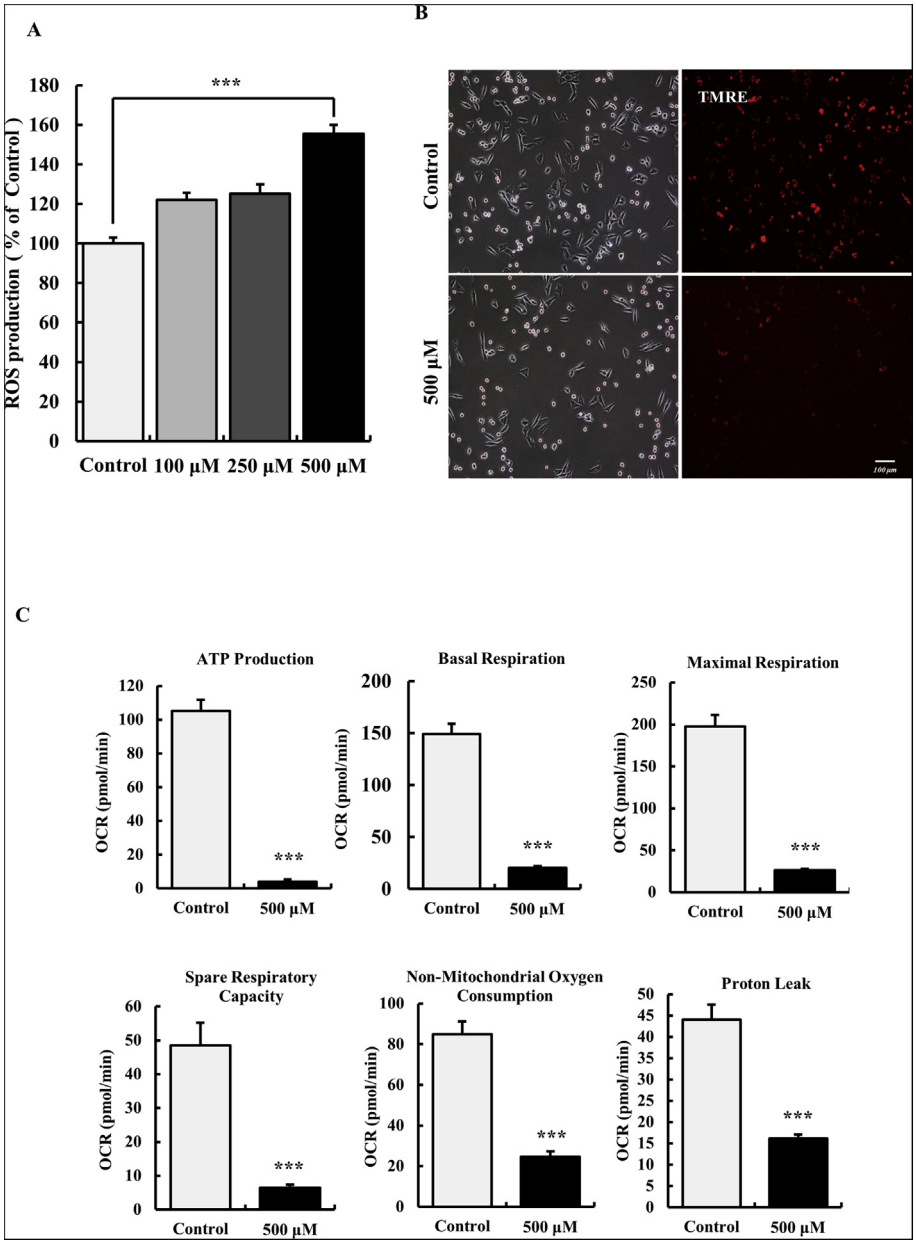

Fig. 3. DBP produced ROS via mitochondria dysfunction in NPCs. (A) Intracellular ROS levels at 6 h after treatment with 500 μM DBP in NPCs cells. Results are presented as means ± standard errors (n = 8). (B) TMRE analysis was performed to determine mitochondrial membrane potential and mitochondrial dysfunction caused by DBP. Scale bar = 100 μm. (C) XF analysis was performed to measure mitochondrial oxygen consumption and determine whether mitochondrial dysfunction had occurred. Results are presented as means ± standard errors (n = 9). $^{***}p < 0.001$ as compared with control (ANOVA with Fisher's PLSD procedure).

microglia marker) and GFAP (an astrocyte marker) in order to determine whether reductions in hippocampal neurogenesis by DBP were associated with neuroinflammation, but no significant effect was observed (Fig. 5D). These observations show DBP impaired hippocampal neurogenesis without affecting neuroinflammatory responses.

3.6. DBP impaired spatial learning and memory in adult mice

It has been reported hippocampal neurogenesis, spatial learning and memory are inter-related (Clelland et al., 2009). To investigate the effect of reduced hippocampal neurogenesis on spatial learning and memory, the MWM test was performed after administering 10 or 50 mg/kg bw DBP i.p. for 2 weeks. Interestingly, latency was significantly increased in mice treated with 50 mg/kg bw of DBP, but not in mice treated with 10 mg/kg bw (Fig. 6A). On the 6th probe test day, the platform was removed and times spent in the quadrant that previously contained the platform were recorded. These 'probe test' results showed that mice administered 50 mg/kg bw DBP spent less time in the target zone than vehicle (Fig. 6B).

4. Discussion

The most worrying reported side effects of DBP are developmental toxicity and reproductive toxicity (Kay et al., 2013). DBP and other phthalates have been shown to penetrate the blood brain and placental barriers in mammals (Huang et al., 2014; Min et al., 2014; Williams and Blanchfield, 1975; Wojtowicz et al., 2018), and phthalates can adversely affect the nervous system by accessing brain tissue through the placental barrier. Neurotoxic studies on DBP have mainly focused on mature neurons and cognitive function, but existing data do not adequately address the neurotoxicity of DBP particularly in developing neurons and NPCs.

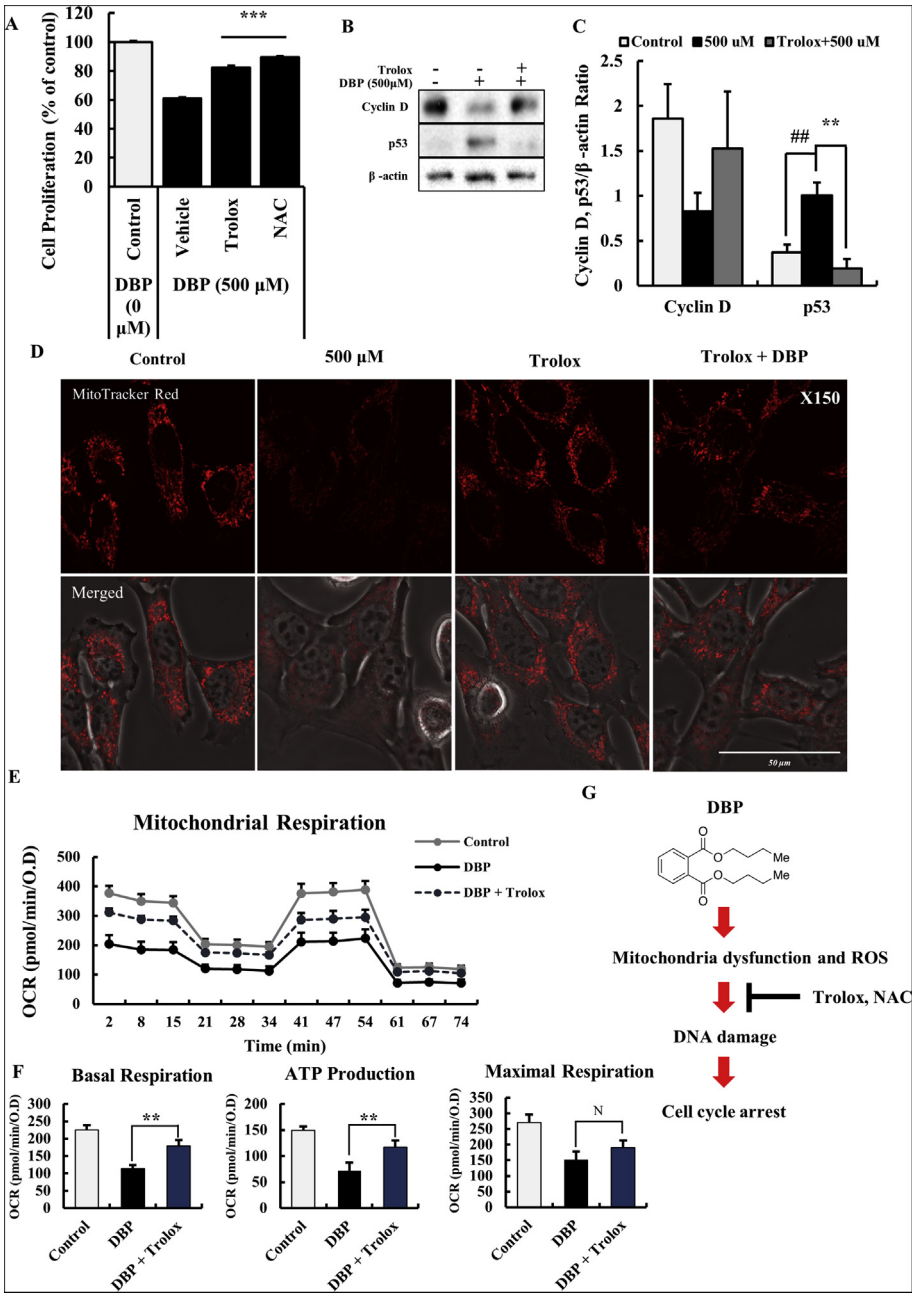

Fig. 4. Antioxidants prevented DBP induced cell cycle arrest. (A) Cell proliferations were measured using a MTT assay in DBP and DBP/trolox co-treatment groups after 6 h of treatment. Results are presented as means ± standard errors (n = 8). (B and C) Western blot analysis was performed to investigate effects on cell cycle arrest marker proteins. A representative blot from three independent experiments that yielded similar results is shown. Quantitative analysis was performed next to the marker. Results are presented as means ± standard errors (n = 3). (D) Mitochondria were labeled using a Mitotracker probe and protected from DBP by trolox. (E and F) XF analysis was performed to measure mitochondrial oxygen consumption and showed DBP induced mitochondrial dysfunction was inhibited by trolox. Results are presented as means ± standard errors (n = 4). (G) The diagram summarizes *in vitro* results. $^{\#\#}p < 0.01$ vs control, $^{**}p < 0.01$, $^{***}p < 0.001$ vs. DBP.

The experimental evidence presented by the present study shows that at high concentration (500 μM) DBP significantly reduces NPC proliferation by causing cell cycle arrest at G1. Previous studies have reported DBP (100 or 1,000 μg/ml) induces cell cycle arrest and apoptosis in mouse ovarian antral follicles (Craig et al., 2013). However, despite reports that the toxic effects of DBP NPCs involve cell cycle arrest, we found no evidence to support DBP-induced apoptosis or necrosis. For example, MTT assays showed DBP reduced cell proliferation, but FACS and PI-Hoechst staining failed to detect changes in the levels of cell death markers.

Cyclin D1 has been reported to be an important regulator of cell cycle progression from G1 to S, and its overexpression has been implicated in cancer progression (Alao, 2007). Cyclin D is an early activator of G1 and forms an active complex with cyclin-dependent kinase that promotes cell cycle progression by phosphorylating and deactivating retinoblastoma protein (Kato et al., 1993; Weinberg, 1995). Cyclin D also begins to rise initially and begins to accumulate at the G1/S boundary (Alao, 2007). Furthermore, abrupt falls in cyclin D levels are predictive of G1 phase arrest (Lanctot et al., 2017). Based on our observations and the above reports, suggesting that DBP caused G1 phase arrest by markedly reducing cyclin D levels (Fig. 2C).

Many studies have shown p53, tumor suppressor and transcription factor, regulates many cellular function including the induction of the expression of genes involved in DNA repair, cell cycle arrest, or apoptosis (Chen, 2016). Most mammalian cells are known to exhibit transient arrest in the G1 and G2 phases after DNA damages, and that p53-dependent G1 arrest provides the time required for DNA repair (Pellegata et al., 1996). In the present study, observed decrease in cyclin D level was interpreted as being indicative of increase in p53 level, but DBP-induced p53 was not responsible for apoptosis. Although one of the major functions of p53 is principally related to the apoptosis, the induction of the p53-mediated checkpoints is triggered by the DNA damage response during the early stages of tumor, and contributes to the suppression of cell proliferation (Meek, 2009). Senturk et al. showed DNA damage induces cell cycle arrest in the G1, S and G2/M phases (Senturk and Manfredi, 2013), and Kuo et al. reported that the

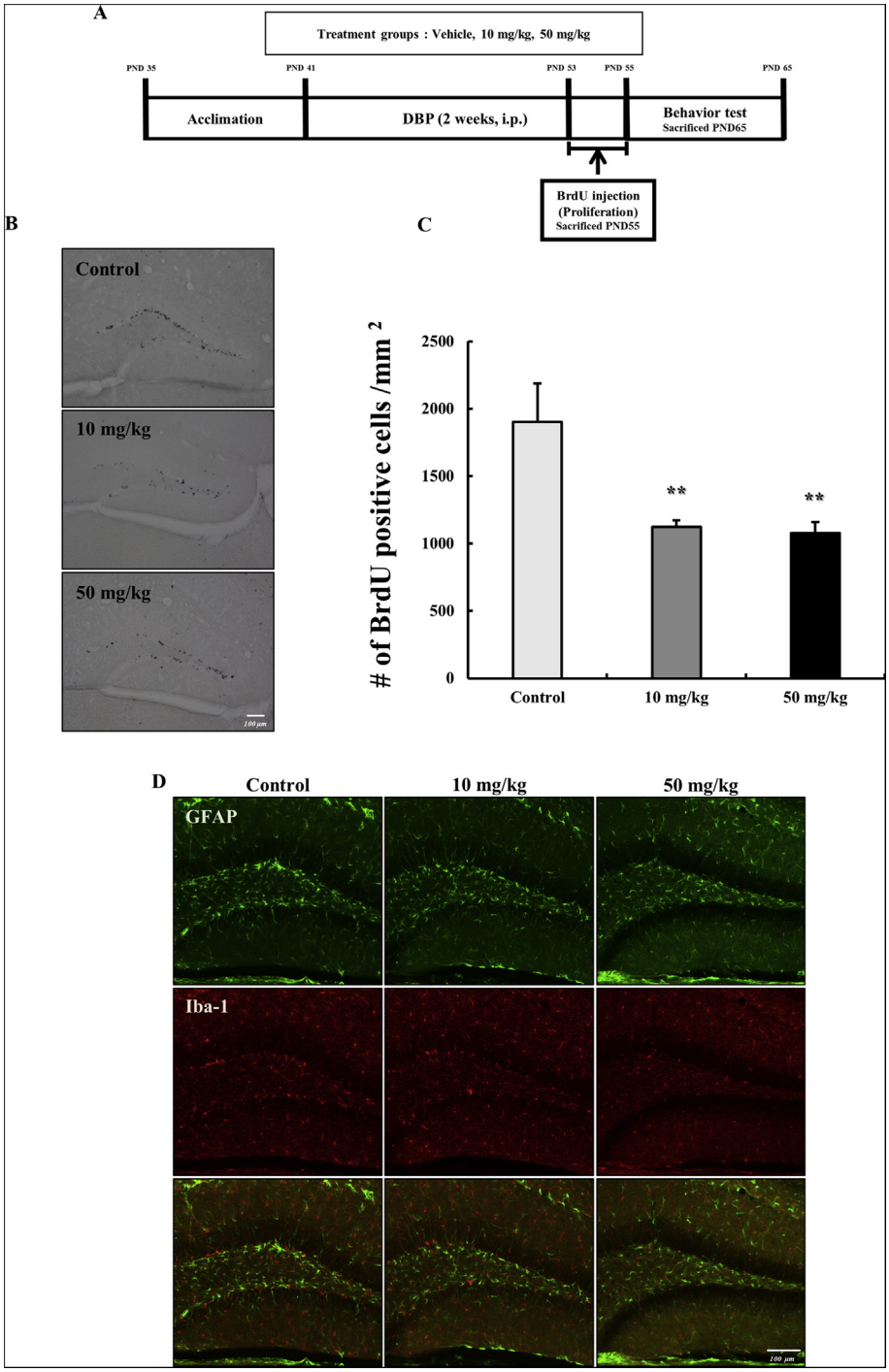

Fig. 5. DBP disrupted hippocampal neurogenesis. (A) *In vivo* experimental design (B and C) Representative images and quantitative analysis showing newly generated neurons in DG. Results are presented as means ± standard errors (n = 5). (D) DBP did not induce neuronal inflammation. Representative image results for GFAP and Iba-1 IHC. Scale bar = 100 μm. $^{**}p < 0.01$ vs. vehicle (determined by ANOVA with Fisher's PLSD procedure).

phosphorylated protein γ-H2AX recruits DNA repair proteins (Kuo and Yang, 2008). In the present study, ICC using γ-H2AX confirmed DNA damage was caused by DBP.

Several studies have shown DBP increases ROS generation (Wojtowicz et al., 2017; Wu et al., 2017), and ROS-induced oxidative stress is known to participate in the pathophysiology of various diseases (Kurien et al., 2006). In addition, oxidative stress can be caused by several subcellular ROS such as peroxisome, ER stress, metabolizing enzymes, radiation, cytokines, and mitochondria, and elevated ROS levels can damage DNA, and thus, cause cell cycle arrest (Abdal Dayem et al., 2017; Barnes, 2015; Schieber and Chandel, 2014). Therefore, concentration-dependent increases in ROS by DBP may have caused the DNA damage and cell cycle arrest observed in the present study. ROS and mitochondrial dysfunction are well-correlated, and oxidative stress responses are induced by mitochondrial dysfunction (Wang et al., 2013). In the present study, mitochondrial dysfunction was observed by TMRE staining and XF analysis after treating NPCs with DBP (Fig. 3). Using antioxidants trolox and NAC to evaluate the roles of ROS in DBP-mediated G1 phase arrest and found that blocking DBP-induced oxidative stress with trolox effectively prevented DBP-induced impaired

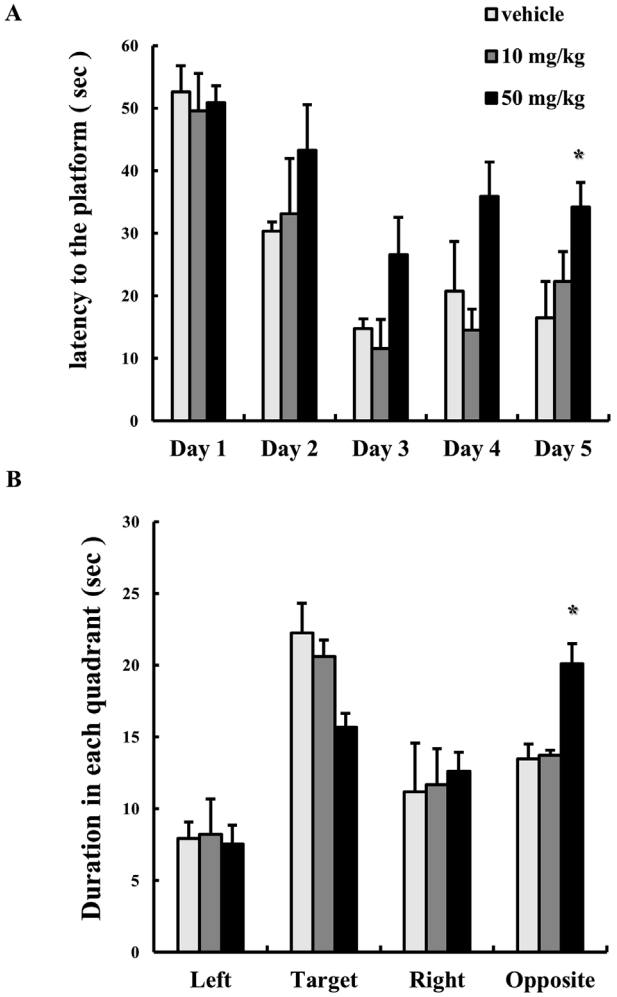

Fig. 6. Evaluation of the effect of DBP on spatial learning and memory. (A) Hidden platform test latencies (times taken to find the platform). (B) Probe test of times spent in each quadrant, which showed DBP impaired memory retention. Results are presented as means ± standard errors (n = 5). $^{*}p < 0.05$ vs. vehicle (ANOVA with Fisher's PLSD procedure).

cell proliferation, cell cycle arrest, and mitochondrial dysfunction (Fig. 4). These observations indicate DBP caused mitochondrial dysfunction and oxidative stress and that this oxidative stress led to DNA damage and cell cycle arrest.

Adult neural stem cells reside in specific regions of brain and continue to proliferate, differentiate, migrate, and produce mature neurons in mammals throughout life (Kempermann et al., 2015). Moreover, the balance between quiescent and activated adult neural stem cells is of considerable importance (Taupin, 2007; Urban and Guillemot, 2014). In the present study, the proliferation of newly generated cells in DG was reduced in mice treated with DBP, and this was supported by our *in vitro* data. Li et al. reported neuronal apoptosis was induced by DBP at 500 mg/kg bw (Li et al., 2013). In the present study, DBP administered at 10 or 50 mg/kg bw did not induce cell death or neuroinflammation, but had significant effects on neural stem cell proliferation in the adult hippocampus, and adult hippocampal neurogenesis has been implicated in learning and memory under normal physiological conditions (Toda et al., 2018). Furthermore, MWM testing showed DBP adversely affected spatial learning and memory and that latencies were significantly greater and times required to find the platform during the probe trial were greater in the 50 mg/kg bw group than in vehicle. Since learning and memory are influenced by neural plasticity as well as hippocampal neurogenesis (Del Olmo et al., 2006; VanGuilder et al., 2011), DBP-mediated memory impairments might be associated with changes in brain plasticity and remodeling induced by external stimulation or learning. In a previous DBP-mediated behavioral study, nuclear condensation and size reductions were observed in DG cells of DBP treated mice, which also exhibited neurobehavioral abnormalities in an open field test and a passive avoidance test (Farzanehfar et al., 2016). Furthermore, Li et al. reported perinatal DBP exposure (at 500 mg/kg bw) impaired spatial learning and memory, and increased apoptosis in hippocampi in offspring rats (Li et al., 2013).

The present study shows DBP at 500 μM induces G1 phase cell cycle arrest in NPCs and that this is mediated by oxidative stress and mitochondrial dysfunction. In addition, our *in vivo* study revealed DBP reduced numbers of newly generated neurons in hippocampi and adversely affected spatial learning and memory. Neural stem cells exist in adult hippocampus and continue to grow in order to maintain hippocampal neurogenesis which is important for forming new memory. Since progression through the G1 phase, which is accompanied by the up-regulations of cellular signaling pathways and protein secretion, is critical for the proliferation of neural stem cells, the cell cycle is important for maintaining adult hippocampal neurogenesis.

Conflict of interest

The authors have no conflict of interest to declare.

Acknowledgements

This research was supported by PNU-RENovation (2018–2019).

This work was also supported by the National Research Foundation of Korea (Grant no. NRF-2018K2A9A2A08000121).

Transparency document

Transparency document related to this article can be found online at https://doi.org/10.1016/j.fct.2019.04.040

Appendix A. Supplementary data

Supplementary data to this article can be found online at https://doi.org/10.1016/j.fct.2019.04.040.

References

Abdal Dayem, A., Hossain, M.K., Lee, S.B., Kim, K., Saha, S.K., Yang, G.M., Choi, H.Y., Cho, S.G., 2017. The role of reactive oxygen species (ROS) in the biological activities of metallic nanoparticles. Int. J. Mol. Sci. 18.

Afshari, A., Gunnarsen, L., Clausen, P.A., Hansen, V., 2004. Emission of phthalates from PVC and other materials. Indoor Air 14, 120–128.

Ait Bamai, Y., Araki, A., Kawai, T., Tsuboi, T., Saito, I., Yoshioka, E., Cong, S., Kishi, R., 2016. Exposure to phthalates in house dust and associated allergies in children aged 6-12years. Environ. Int. 96, 16–23.

Alao, J.P., 2007. The regulation of cyclin D1 degradation: roles in cancer development and the potential for therapeutic invention. Mol. Canc. 6, 24.

Barnes, P.J., 2015. Mechanisms of development of multimorbidity in the elderly. Eur. Respir. J. 45, 790–806.

Chen, J., 2016. The cell-cycle arrest and apoptotic functions of p53 in tumor initiation and progression. Cold Spring Harb Perspect Med 6, a026104.

Cho, J.H., Kim, A.H., Lee, S., Lee, Y., Lee, W.J., Chang, S.C., Lee, J., 2018. Sensitive neurotoxicity assessment of bisphenol A using double immunocytochemistry of DCX and MAP2. Arch Pharm. Res. (Seoul) 41, 1098–1107.

Clelland, C.D., Choi, M., Romberg, C., Clemenson Jr., G.D., Fragniere, A., Tyers, P., Jessberger, S., Saksida, L.M., Barker, R.A., Gage, F.H., Bussey, T.J., 2009. A functional role for adult hippocampal neurogenesis in spatial pattern separation. Science 325, 210–213.

Craig, Z.R., Hannon, P.R., Wang, W., Ziv-Gal, A., Flaws, J.A., 2013. Di-n-butyl phthalate disrupts the expression of genes involved in cell cycle and apoptotic pathways in mouse ovarian antral follicles. Biol. Reprod. 88, 23.

Del Olmo, N., Higuera-Matas, A., Miguens, M., Garcia-Lecumberri, C., Borcel, E., Solis, J.M., Ambrosio, E., 2006. Hippocampal synaptic plasticity and water maze learning in cocaine self-administered rats. Ann. N. Y. Acad. Sci. 1074, 427–437.

Ding, Y., Lu, L., Xuan, C., Han, J., Ye, S., Cao, T., Chen, W., Li, A., Zhang, X., 2017. Di-n-butyl phthalate exposure negatively influences structural and functional

neuroplasticity via Rho-GTPase signaling pathways. Food Chem. Toxicol. 105, 34–43.
Farzanehfar, V., Naderi, N., Kobarfard, F., Faizi, M., 2016. Determination of dibutyl phthalate neurobehavioral toxicity in mice. Food Chem. Toxicol. 94, 221–226.
Hauser, R., Calafat, A.M., 2005. Phthalates and human health. Occup. Environ. Med. 62, 806–818.
Hauser, R., Meeker, J.D., Park, S., Silva, M.J., Calafat, A.M., 2004. Temporal variability of urinary phthalate metabolite levels in men of reproductive age. Environ. Health Perspect. 112, 1734–1740.
Huang, Y., Li, J., Garcia, J.M., Lin, H., Wang, Y., Yan, P., Wang, L., Tan, Y., Luo, J., Qiu, Z., Chen, J.A., Shu, W., 2014. Phthalate levels in cord blood are associated with preterm delivery and fetal growth parameters in Chinese women. PLoS One 9, e87430.
Jang, Y.J., Park, H.R., Kim, T.H., Yang, W.J., Lee, J.J., Choi, S.Y., Oh, S.B., Lee, E., Park, J.H., Kim, H.P., Kim, H.S., Lee, J., 2012. High dose bisphenol A impairs hippocampal neurogenesis in female mice across generations. Toxicology 296, 73–82.
Kamrin, M.A., 2009. Phthalate risks, phthalate regulation, and public health: a review. J. Toxicol. Environ. Health B Crit. Rev. 12, 157–174.
Kato, J., Matsushime, H., Hiebert, S.W., Ewen, M.E., Sherr, C.J., 1993. Direct binding of cyclin D to the retinoblastoma gene product (pRb) and pRb phosphorylation by the cyclin D-dependent kinase CDK4. Genes Dev. 7, 331–342.
Kay, V.R., Chambers, C., Foster, W.G., 2013. Reproductive and developmental effects of phthalate diesters in females. Crit. Rev. Toxicol. 43, 200–219.
Kempermann, G., Song, H., Gage, F.H., 2015. Neurogenesis in the adult Hippocampus. Cold Spring Harb Perspect Biol 7, a018812.
Kobrosly, R.W., Evans, S., Miodovnik, A., Barrett, E.S., Thurston, S.W., Calafat, A.M., Swan, S.H., 2014. Prenatal phthalate exposures and neurobehavioral development scores in boys and girls at 6-10 years of age. Environ. Health Perspect. 122, 521–528.
Koch, H.M., Calafat, A.M., 2009. Human body burdens of chemicals used in plastic manufacture. Philos. Trans. R. Soc. Lond. B Biol. Sci. 364, 2063–2078.
Kuo, L.J., Yang, L.X., 2008. Gamma-H2AX - a novel biomarker for DNA double-strand breaks. In Vivo 22, 305–309.
Kurien, B.T., Hensley, K., Bachmann, M., Scofield, R.H., 2006. Oxidatively modified autoantigens in autoimmune diseases. Free Radic. Biol. Med. 41, 549–556.
Lanctot, A.A., Guo, Y., Le, Y., Edens, B.M., Nowakowski, R.S., Feng, Y., 2017. Loss of brap results in premature G1/S phase transition and impeded neural progenitor differentiation. Cell Rep. 20, 1148–1160.
Lee, S., Park, H.R., Lee, J.Y., Cho, J.H., Song, H.M., Kim, A.H., Lee, W., Lee, Y., Chang, S.C., Kim, H.S., Lee, J., 2018. Learning, memory deficits, and impaired neuronal maturation attributed to acrylamide. J. Toxicol. Environ. Health 81, 254–265.
Li, X.J., Jiang, L., Chen, L., Chen, H.S., Li, X., 2013. Neurotoxicity of dibutyl phthalate in brain development following perinatal exposure: a study in rats. Environ. Toxicol. Pharmacol. 36, 392–402.
Li, Y., Zhuang, M., Li, T., Shi, N., 2009. Neurobehavioral toxicity study of dibutyl phthalate on rats following in utero and lactational exposure. J. Appl. Toxicol. 29, 603–611.
Maestre-Batlle, D., Pena, O.M., Huff, R.D., Randhawa, A., Carlsten, C., Bolling, A.K., 2018. Dibutyl phthalate modulates phenotype of granulocytes in human blood in response to inflammatory stimuli. Toxicol. Lett. 296, 23–30.
Meek, D.,W., 2009. Tumor suppression by p53: a role for the DNA damage response? Nat. Rev. Canc. 9 (10), 714–723.
Min, A., Liu, F., Yang, X., Chen, M., 2014. Benzyl butyl phthalate exposure impairs learning and memory and attenuates neurotransmission and CREB phosphorylation in mice. Food Chem. Toxicol. 71, 81–89.
Pellegata, N.S., Antoniono, R.J., Redpath, J.L., Stanbridge, E.J., 1996. DNA damage and p53-mediated cell cycle arrest: a reevaluation. Proc. Natl. Acad. Sci. U. S. A. 93, 15209–15214.
Pivnenko, K., Eriksen, M.K., Martin-Fernandez, J.A., Eriksson, E., Astrup, T.F., 2016. Recycling of plastic waste: presence of phthalates in plastics from households and industry. Waste Manag. 54, 44–52.
Riss, T., Hook, B., Duellman, S., 2015. Evaluation of real time cell viability assays multiplexed with other methods. Toxicol. Lett. 238, S179–S180.
Schecter, A., Lorber, M., Guo, Y., Wu, Q., Yun, S.H., Kannan, K., Hommel, M., Imran, N., Hynan, L.S., Cheng, D., Colacino, J.A., Birnbaum, L.S., 2013. Phthalate concentrations and dietary exposure from food purchased in New York State. Environ. Health Perspect. 121, 473–494.
Schettler, T., 2006. Human exposure to phthalates via consumer products. Int. J. Androl. 29, 134–139 discussion 181-135.
Schieber, M., Chandel, N.S., 2014. ROS function in redox signaling and oxidative stress. Curr. Biol. 24, R453–R462.
Senturk, E., Manfredi, J.J., 2013. p53 and cell cycle effects after DNA damage. Methods Mol. Biol. 962, 49–61.
Shukitt-Hale, B., Carey, A.N., Jenkins, D., Rabin, B.M., Joseph, J.A., 2007. Beneficial effects of fruit extracts on neuronal function and behavior in a rodent model of accelerated aging. Neurobiol. Aging 28, 1187–1194.
Snyder, E.Y., Deitcher, D.L., Walsh, C., Arnold-Aldea, S., Hartwieg, E.A., Cepko, C.L., 1992. Multipotent neural cell lines can engraft and participate in development of mouse cerebellum. Cell 68, 33–51.
Struve, M.F., Gaido, K.W., Hensley, J.B., Lehmann, K.P., Ross, S.M., Sochaski, M.A., Willson, G.A., Dorman, D.C., 2009. Reproductive toxicity and pharmacokinetics of di-n-butyl phthalate (DBP) following dietary exposure of pregnant rats. Birth Defects Res B Dev Reprod Toxicol 86, 345–354.
Taupin, P., 2007. BrdU immunohistochemistry for studying adult neurogenesis: paradigms, pitfalls, limitations, and validation. Brain Res. Rev. 53, 198–214.
Thompson, R.C., Swan, S.H., Moore, C.J., vom Saal, F.S., 2009. Our plastic age. Philos. Trans. R. Soc. Lond. B Biol. Sci. 364, 1973–1976.
Tiwari, S.K., Agarwal, S., Tripathi, A., Chaturvedi, R.K., 2016. Bisphenol-a mediated inhibition of hippocampal neurogenesis attenuated by curcumin via canonical wnt pathway. Mol. Neurobiol. 53, 3010–3029.
Toda, T., Parylak, S.L., Linker, S.B., Gage, F.H., 2018. The role of adult hippocampal neurogenesis in brain health and disease. Mol. Psychiatr. 24, 67–87.
Urban, N., Guillemot, F., 2014. Neurogenesis in the embryonic and adult brain: same regulators, different roles. Front. Cell. Neurosci. 8, 396.
VanGuilder, H.D., Farley, J.A., Yan, H., Van Kirk, C.A., Mitschelen, M., Sonntag, W.E., Freeman, W.M., 2011. Hippocampal dysregulation of synaptic plasticity-associated proteins with age-related cognitive decline. Neurobiol. Dis. 43, 201–212.
Wang, C.H., Wu, S.B., Wu, Y.T., Wei, Y.H., 2013. Oxidative stress response elicited by mitochondrial dysfunction: implication in the pathophysiology of aging. Exp. Biol. Med. 238, 450–460.
Weinberg, R.A., 1995. The retinoblastoma protein and cell cycle control. Cell 81, 323–330.
Williams, D.T., Blanchfield, B.J., 1975. The retention, distribution, excretion, and metabolism of dibutyl phthalate-7-14 C in the rat. J. Agric. Food Chem. 23, 854–858.
Wojtowicz, A.K., Sitarz-Glownia, A.M., Szczesna, M., Szychowski, K.A., 2018. The action of di-(2-ethylhexyl) phthalate (DEHP) in mouse cerebral cells involves an impairment in aryl hydrocarbon receptor (AhR) signaling. Neurotox. Res. 35, 183–195.
Wojtowicz, A.K., Szychowski, K.A., Wnuk, A., Kajta, M., 2017. Dibutyl phthalate (DBP)-Induced apoptosis and neurotoxicity are mediated via the aryl hydrocarbon receptor (AhR) but not by estrogen receptor alpha (ERalpha), estrogen receptor beta (ERbeta), or peroxisome proliferator-activated receptor gamma (PPARgamma) in mouse cortical neurons. Neurotox. Res. 31, 77–89.
Wormuth, M., Scheringer, M., Vollenweider, M., Hungerbuhler, K., 2006. What are the sources of exposure to eight frequently used phthalic acid esters in Europeans? Risk Anal. 26, 803–824.
Wu, Y., Li, J., Yan, B., Zhu, Y., Liu, X., Chen, M., Li, D., Lee, C.C., Yang, X., Ma, P., 2017. Oral exposure to dibutyl phthalate exacerbates chronic lymphocytic thyroiditis through oxidative stress in female Wistar rats. Sci. Rep. 7, 15469.
Xiao, W., Jiang, Y., Men, Q., Yuan, L., Huang, Z., Liu, T., Li, W., Liu, X., 2015. Tetrandrine induces G1/S cell cycle arrest through the ROS/Akt pathway in EOMA cells and inhibits angiogenesis in vivo. Int. J. Oncol. 46, 360–368.
Xu, H., Shao, X., Zhang, Z., Zou, Y., Chen, Y., Han, S., Wang, S., Wu, X., Yang, L., Chen, Z., 2013. Effects of di-n-butyl phthalate and diethyl phthalate on acetylcholinesterase activity and neurotoxicity related gene expression in embryonic zebrafish. Bull. Environ. Contam. Toxicol. 91, 635–639.
Xu, W., You, Y., Wang, Z., Chen, W., Zeng, J., Zhao, X., Su, Y., 2018. Dibutyl phthalate alters the metabolic pathways of microbes in black soils. Sci. Rep. 8, 2605.